Automata network predator-prey model with pursuit and evasion

N. Boccara,[1,2] O. Roblin,[1,3] and M. Roger[1]

[1] *Direction des Sciences de la Matière Département de Recherche sur l'Etat Condensé, les Atomes, les Molécules–Service de Physique de l'Etat Condensé, Commissariat à l'Energie Atomique, Centre d'Etudes de Saclay, 91191 Gif-sur-Yvette Cedex, France*

[2] *Department of Physics, University of Illinois, Chicago, Illinois 60607-7059*

[3] *Ecole Supérieure d'Electricité, 91192 Gif-sur-Yvette Cedex, France*

(Received 21 June 1994)

An automata network predator-prey model with pursuit and evasion is studied. The local rule consists of two subrules. The first, applied synchronously, models predation, birth, and death processes. The second, applied sequentially, describes predator pursuit to catch evading preys. The model contains six parameters: the birth and death rates of preys and predators and two parameters characterizing the motion of preys and predators. The model has three fixed points. The first is trivial; it corresponds to a stationary state with no living individuals. The second characterizes a state with no predators. The third describes a state with nonzero densities of preys and predators. Moreover, the model may exhibit oscillatory behavior of the local prey and predator densities as functions of time through a Hopf bifurcation. In this particular case spatial coherence is lost. Spatial correlations decay with a finite correlation length ξ. Although local densities, measured over a range of the order of ξ, oscillate, collective variables are stationary.

PACS number(s): 05.45.+b, 05.50.+q

I. INTRODUCTION

Since Volterra [1] published the first simple predator-prey model to explain the oscillatory levels of certain fish catches in the Adriatic, a rich variety of models has been proposed. Murray's book [2] is a good introduction to this fast-growing literature.

This paper discusses a rather general predator-prey model. It is formulated in terms of automata networks [3,4], which describe more correctly the local character of predation than differential equations. An automata network is a graph with a discrete variable at each vertex which evolves in discrete time steps according to a definite rule involving the values of neighboring vertex variables. The vertex variables may be updated sequentially or synchronously.

Automata networks are discrete dynamical systems, which may be defined more formally as follows. Let $G = (V, E)$ be a graph, where V is a set of vertices and E a set of edges. Each edge joins two vertices not necessarily distinct. An automata network, defined on V, is a triple $(G, Q, \{f_i | i \in V\})$, where G is a graph on V, Q a finite set of states and $f_i: Q^{|U_i|} \rightarrow Q$ a mapping, called the local transition rule associated to vertex i. $U_i = \{j \in V | \{j, i\} \in E\}$ is the neighborhood of i, i.e., the set of vertices connected to i, and $|U_i|$ denotes the number of vertices belonging to U_i. The graph G is assumed to be locally finite, i.e., for all $i \in V$, $|U_i| < \infty$.

In our model, the set V is the two-dimensional torus $\mathbf{Z}_L^2$, where $\mathbf{Z}_L$ is the set of integers modulo L. A vertex is either empty or occupied by either a *predator*, or a *prey*. In what follows, according to the process under consideration, we will consider two different neighborhoods. The *predation neighborhood* consists of the four nearest neighbors of a given site, whereas the *pursuit and evasion neighborhood* consists of a Moore-type neighborhood which contains $(2r + 1)^2 - 1$ sites ($r = 1, 2, ...$, is the range of the *pursuit and evasion neighborhood*).

The evolution of these two populations is governed by the following rules.

(1) A prey has a probability d_h of being captured and eaten by each predator in its predation neighborhood.

(2) If there are no predators in its predation neighborhood, a prey has a probability b_h of giving birth to a prey at an empty neighboring site.

(3) After having eaten a prey, a predator has a probability b_p of giving birth to a predator at the site previously occupied by the prey.

(4) A predator has a probability d_p of dying.

(5) Predators move to catch preys, and preys move to evade predators. The *pursuit and evasion neighborhood* is divided into four quarters. A predator (or prey) at the frontier between two quarters is equally divided between the two quarters. Predators move to a first neighboring site in the direction of the highest local prey density. In case of equal highest density in two or four directions, one of them is chosen at random. If three directions correspond to the same highest density the predator selects the middle one. Preys move to a first neighboring site in the direction opposite to the highest predator density. If the four directions are equivalent, one is selected at random. If three directions correspond to the same maximum predator density, preys choose the remaining one. If two directions correspond to an equal highest density, preys choose at random one of the two others. For r larger than 1, if the selected site belongs to the predation neighborhood of a predator, preys do not move. If $N = L^2$ is the total number of sites of $\mathbf{Z}_L^2$, and P (respectively, H) the predator (respectively, prey) density, $m_p PN$ (respectively, $m_h HN$) predators (respectively, preys) are sequentially selected at random to perform a move [for each individual move, a predator or a

prey is chosen with probability $p_0 = m_p P/(m_p P + m_h H)$ or $(1 - p_0)$, respectively]. This sequential process allows some individuals to move more than others. Since an individual may only move to an empty site, the parameters m_p and m_h, which are positive numbers, represent average numbers of *tentative* moves per individual during a unit of time.

Rules 1, 2, 3, and 4 are applied *simultaneously.* Predation, birth and death processes are, therefore, modeled by a three-state two-dimensional cellular automaton rule. Rule 5 is applied *sequentially.* Our model may be viewed as an automata network with a mixed transition rule. At each time step, the evolution results from the application of the synchronous subrule followed by the sequential one.

II. MEAN-FIELD APPROXIMATION

The mean-field approximation ignores space dependence and neglects correlations. It assumes that the probability that either a predator or a prey occupies a lattice site is proportional to the density of the corresponding population. In lattice models with local interactions, quantitative predictions of such an approximation are not very good. However, it can give interesting information on the qualitative behavior of the system in the limit $m_p = m_h \to \infty$.

Let $P(t)$ and $H(t)$ denote the densities at time t of, respectively, predators and prey. We have

$$\begin{aligned} P(t+1) &= F_1(P(t), H(t)) \\ &= P(t) - d_p P(t) + b_p H(t) f(1, d_h P(t)), \qquad (2.1) \\ H(t+1) &= F_2(P(t), H(t)) \\ &= H(t) - H(t) f(1, d_h P(t)) \\ &\quad + [1 - H(t) - P(t)] f(1 - P(t), b_h H(t)), \qquad (2.2) \end{aligned}$$

where the function f is defined by

$$f(p_1, p_2) = p_1^4 - (p_1 - p_2)^4. \qquad (2.3)$$

The expression of $f(p_1, p_2)$ is easy to derive. If $p_2 = d_h P(t)$, then p_2 represents the probability that, at time t, a prey is eaten by a predator located at a specific site of the predation neighborhood. Then $1-(1-p_2)^4 = f(1, p_2)$ is the probability that, at time t, a prey is eaten by a predator located at any of the four sites of the predation neighborhood. If $p_1 = 1 - P(t)$ and $p_2 = b_h H(t)$, then p_1 represents the probability that, at time t, a specific site is not occupied by a predator and p_2 the probability that, at time t, a prey gives birth to a prey at a specific site. Then $p_1^4 - (p_1 - p_2)^4 = f(p_1, p_2)$ is the probability that a prey gives birth to a prey at any of the four sites of the predation neighborhood if there are no predators in this neighborhood. Note that, within the framework of this approximation, the interaction terms are not bilinear as in most population dynamics models [5–7]. Nonbilinear interaction have recently been shown to exhibit very different dynamic behaviors [8].

The fixed points are the solutions of the equations

$$b_p H f(1, d_h P) - d_p P = 0, \qquad (2.4)$$

$$(1 - H - P) f(1 - P, b_h H) - H(t) f(1, d_h P) = 0. \qquad (2.5)$$

These fixed points are stable if the absolute value of the eigenvalues $\lambda_1(H, P)$ and $\lambda_2(H, P)$ of the Jacobian matrix

$$\mathbf{J}(H, P) = \begin{bmatrix} \frac{\partial F_1}{\partial H} & \frac{\partial F_1}{\partial P} \\ \frac{\partial F_2}{\partial H} & \frac{\partial F_2}{\partial P} \end{bmatrix} \qquad (2.6)$$

are less than 1.

Since $f(1, 0) = 0$, $P = 0$ is a solution of Eq. (2.4). In this case Eq. (2.5) can have two different solutions, either $H = 0$ or $H = 1$. The solution $(0, 0)$ is always unstable if $b_h \neq 0$. The solution $(0, 1)$ is stable if the condition $d_p - 4 b_p d_h > 0$ is satisfied.

If $P \neq 0$, Eqs. (2.4) and (2.5) may have another solution which will be denoted (H^*, P^*). The expression of the Jacobian matrix $\mathbf{J}(H^*, P^*)$ is rather complicated and it is easier to study numerically the stability of this fixed point. An interesting feature of the model is that (H^*, P^*) may lose its stability, and a limit cycle becomes stable through a Hopf bifurcation. Figure 1(a) represents a limit cycle obtained within the mean-field approximation for the values $b_p = 0.6$, $d_p = 0.2$, $b_h = 0.2$, and $d_h = 0.9$. Figure 1(b) represents a nontrivial fixed point obtained with a lower birth probability $b_p = 0.2$ for the predators, the three other parameters are unchanged.

III. SIMULATIONS

A. Pursuit and evasion

It is interesting to first examine the influence of the motion (Rule 5), independently of the *predation* law (Rules 1–4). Figure 2 represents patterns obtained with $r = 2$ after $m_p = m_h = 10\,000$ tentative moves, starting with equal number of predator and prey ($H_0 = P_0 = 0.1$) distributed at random. Only the pursuit-evasion process (Rule 5) is applied. In all patterns, predators (respectively, preys) are represented by black (respectively, white) squares on a gray background. As expected, there is a tendency to form small clusters with predators surrounding one or a few preys and preventing them from escape. The remaining preys then move more or less randomly, with the constraint that they should avoid those clusters. Similar patterns have been obtained at large time with very different motion rates (as $m_h/m_p = 100$). For nonequal rates, the main difference is in the time necessary for predators to build clusters around preys. The mean size of these clusters is weakly dependent on m_h/m_p.

B. Simulations with $r = 1$

The influence of motion is emphasized with two sets of parameters for the *predation* law: the former leading to a nontrivial fixed point in mean-field approximation [Fig. 1(b)], the latter corresponding to a cyclic behavior [Fig. 1(a)].

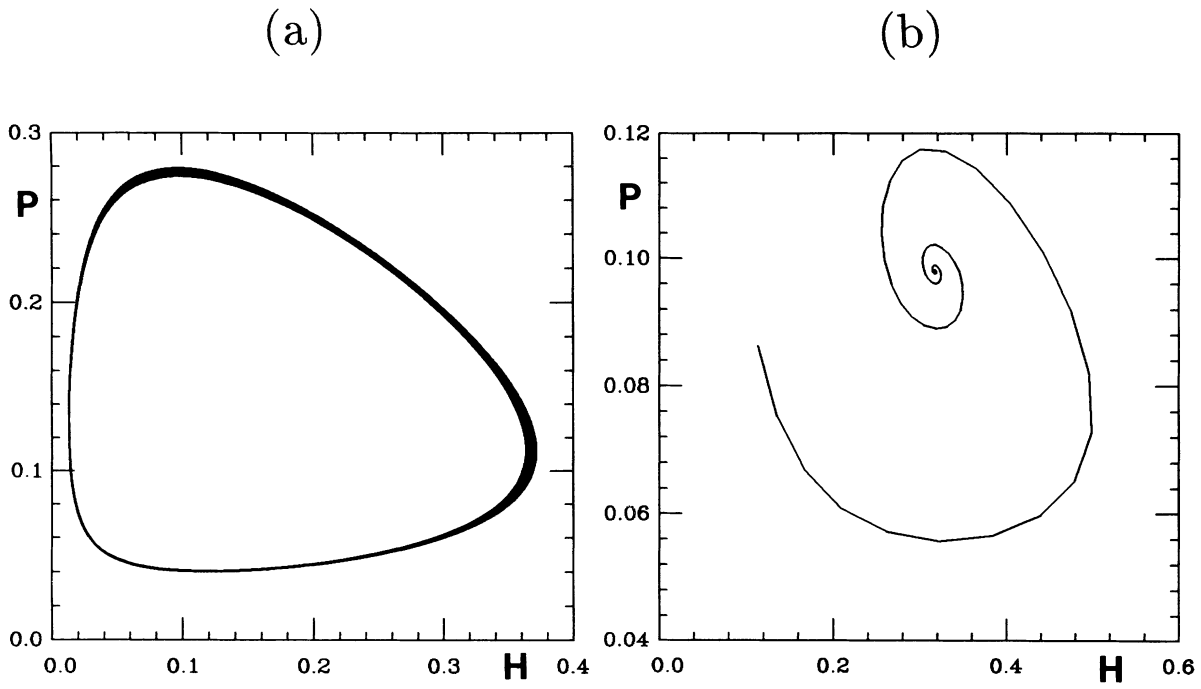

FIG. 1. Mean-field approximation. (a) Stable limit cycle obtained with $b_p = 0.6$, $d_p = 0.2$, $b_h = 0.2$, and $d_h = 0.9$. (b) Fixed point obtained with $b_p = 0.2$, $d_p = 0.2$, $b_h = 0.2$, and $d_h = 0.9$.

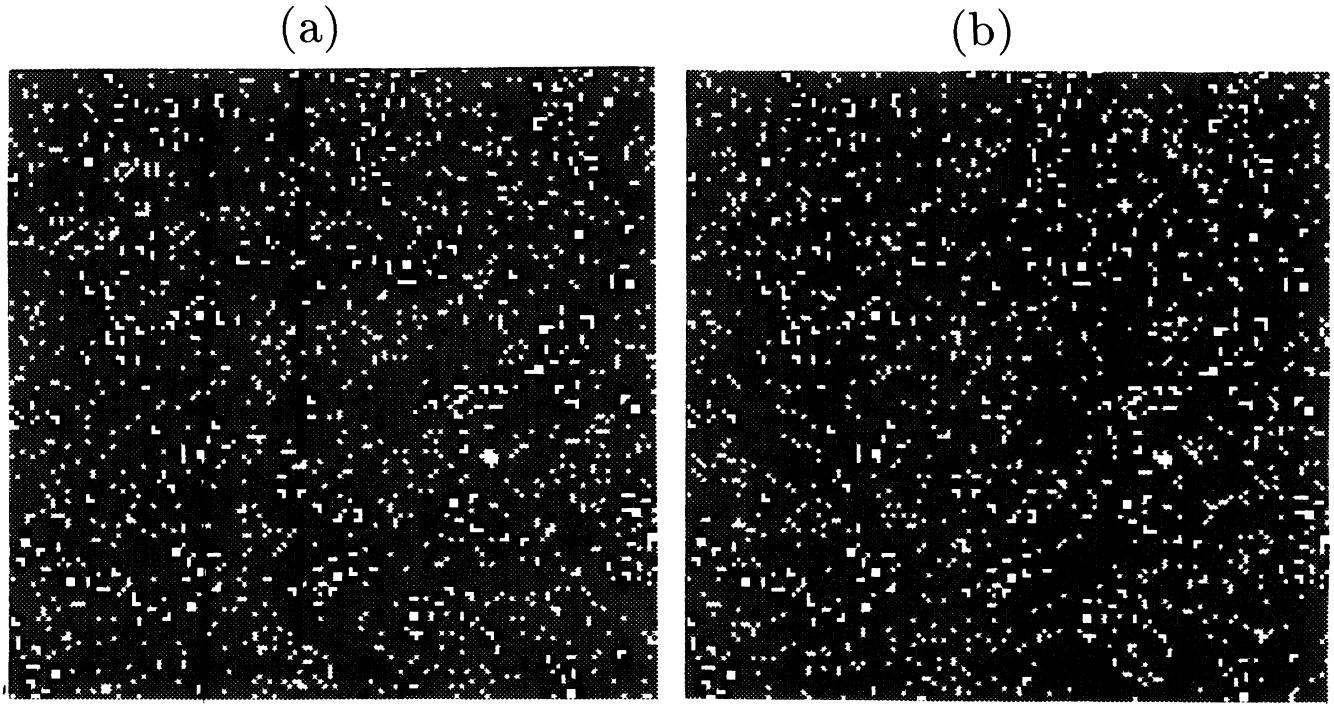

FIG. 2. Patterns obtained after 10 000 and 10 100 tentative moves of predators and preys, starting from an equal concentration $c = 10\%$ of predators and preys distributed at random. Only the *pursuit and evasion process is applied.* In all patterns, predators (respectively, preys) are represented by black (respectively, white) squares on a gray background.

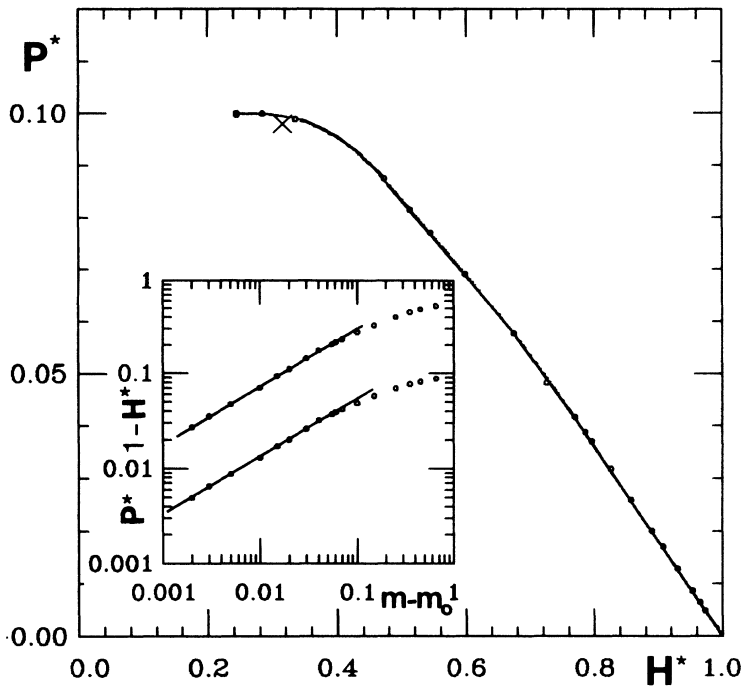

FIG. 3. Variations of the fixed point (H^*, P^*) for $m = m_p = m_h$ going from $m = m_0$ to 500. Here, $b_p = 0.2$, $d_p = 0.2$, $b_h = 0.2$, and $d_h = 0.9$. The cross indicates the mean-field expectation. The inset shows the behavior of $(1 - H^*)$ and P^* close to the critical value $m_0 = 0.350$.

1. *Typical example giving a nontrivial fixed point: $b_p = 0.2$, $d_p = 0.2$, $b_h = 0.2$, $d_h = 0.9$*

We first study the behavior of this automata network, for $m_p = m_h = m$, as a function of m. There is a threshold $m = m_0$ below which the trivial fixed point $(H^* = 1, P^* = 0)$ is obtained. For $m > m_0$, the stationary state when $t \to \infty$ corresponds to a nontrivial fixed point. The evolution of this fixed point (H^*, P^*), for m varying from m_0 to 500 is shown in Fig. 3. The

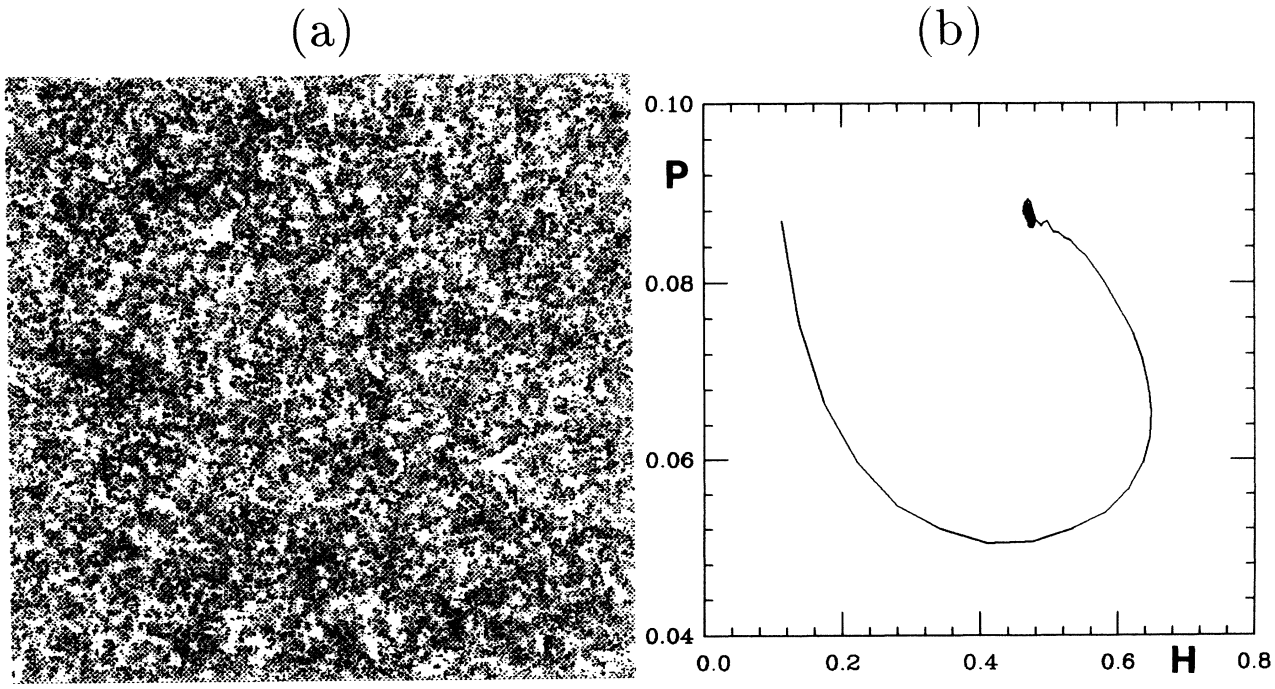

FIG. 4. (a) Patterns obtained after a few hundred time steps, starting from a random distribution of 10% of predators and 10% of preys on a 512×512 lattice with $m_p = m_h = 1$. (b) Corresponding time evolution of the densities (H, P). Here $b_p = 0.2$, $d_p = 0.2$, $b_h = 0.2$, and $d_h = 0.9$.

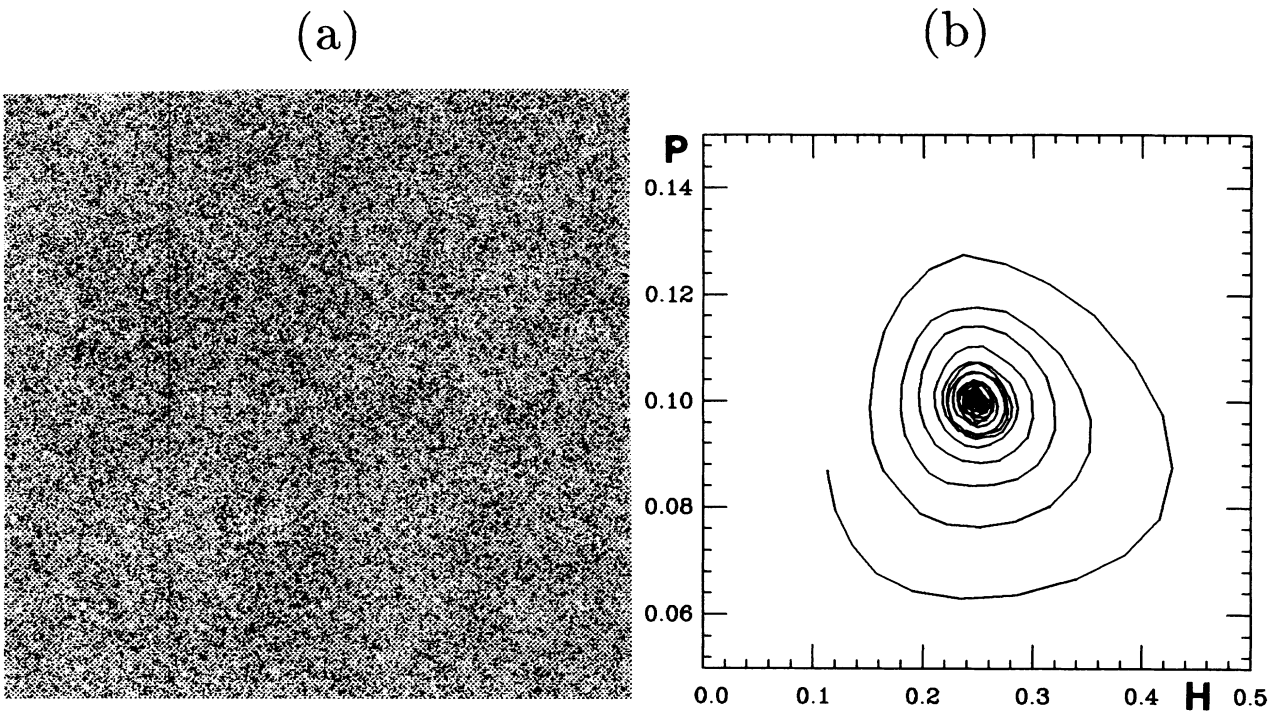

FIG. 5. Same as Fig. 4 with $m_p = m_h = 100$.

cross represents the mean-field prediction $(0.317, 0.098)$, which would be exact for random moves at $m \to \infty$. As expected, since the *pursuit and evasion* moves are not random, the mean-field approximation only gives the qualitative behavior.

For m close to m_0, $(1 - H^*)$ and P^* behave as $(m - m_0)^\beta$ with $m_0 = 0.350 \pm 0.001$ and $\beta = 0.60 \pm 0.02$ (see inset). This value is in reasonable agreement with

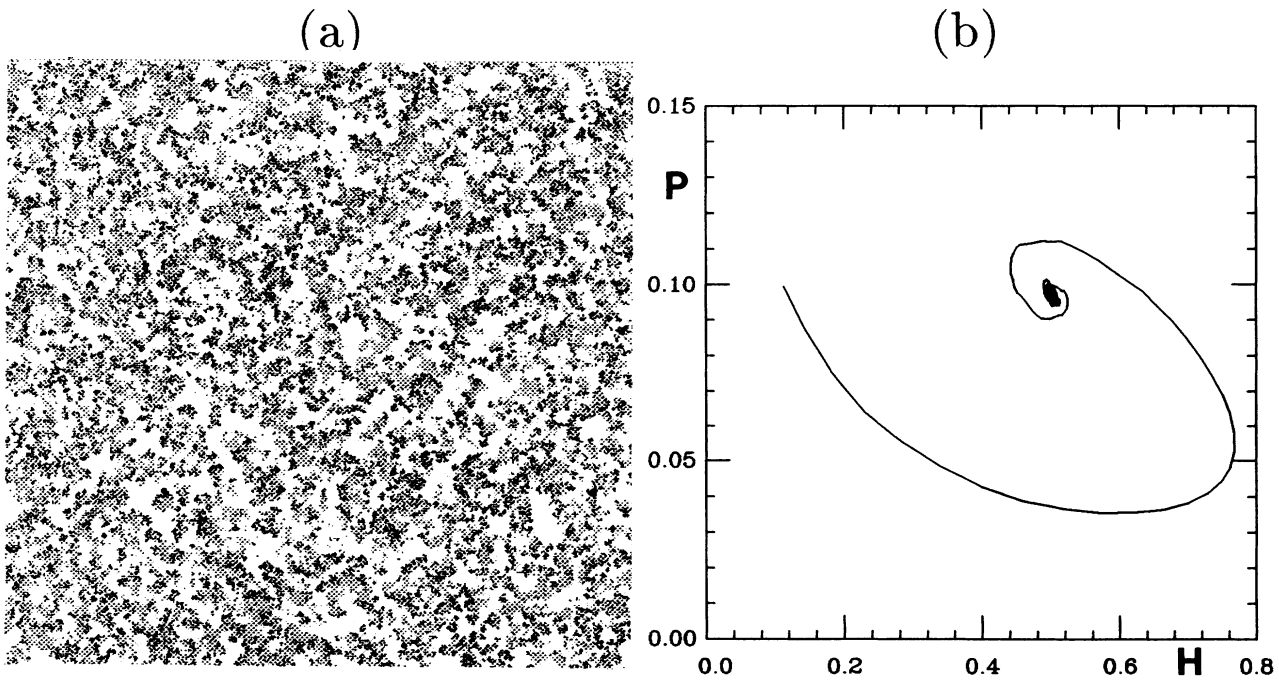

FIG. 6. (a) Pattern obtained after about a few hundred time steps, starting from a random distribution of 10% of predators and 10% of preys on a 512×512 lattice. (b) Time evolution of the densities H, P. Here $b_p = 0.6$, $d_p = 0.2$, $b_h = 0.2$, and $d_h = 0.9$; $m = m_p = m_h = 0.02$.

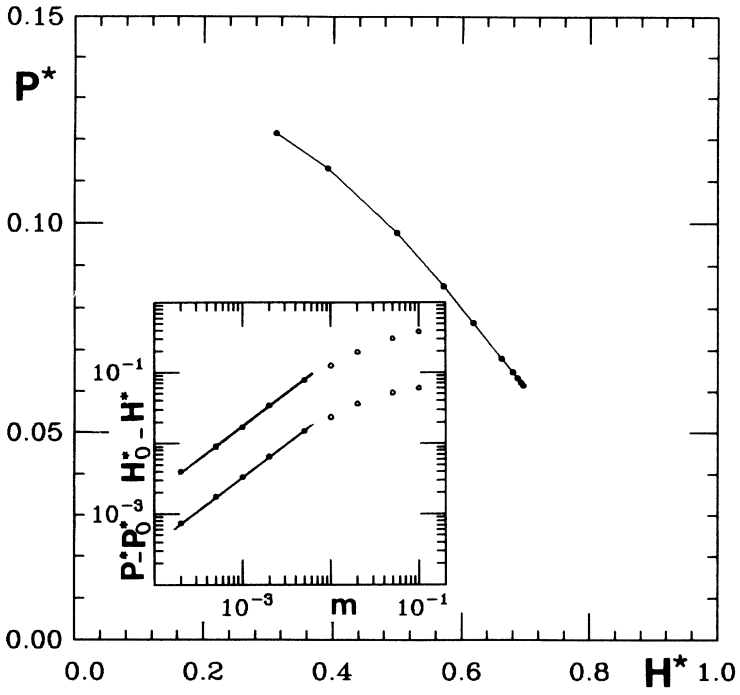

FIG. 7. Variations of the fixed point (H^*, P^*) as a function of $m = m_p = m_h$. Here, $b_p = 0.6$, $d_p = 0.2$, $b_h = 0.2$, and $d_h = 0.9$. The inset shows the behavior of $(H_0^* - H^*)$ and $(P^* - P_0^*)$ for $m \to 0$.

the critical exponent of the two-dimensional directed percolation, as expected, since the predation density plays the role of the order parameter as the density of wet sites in directed percolation.

Figure 4(a) represents a typical pattern obtained after a few hundred of time steps with $m = 1$ and Fig. 4(b) the evolution in the (H, P) plane as a function of time, starting from a random configuration with equal concentration (10%) of preys and predators at $t = 0$. Figure 5 represents a pattern obtained in the same conditions with $m = 100$

2. *Local cyclic behavior:* $b_p = 0.6$, $d_p = 0.2$, $b_h = 0.2$, $d_h = 0.9$

With this set of parameters, allowing a higher predator birth rate b_p, a nontrivial fixed point $(H_0^* = 0.696, P_0^* =$

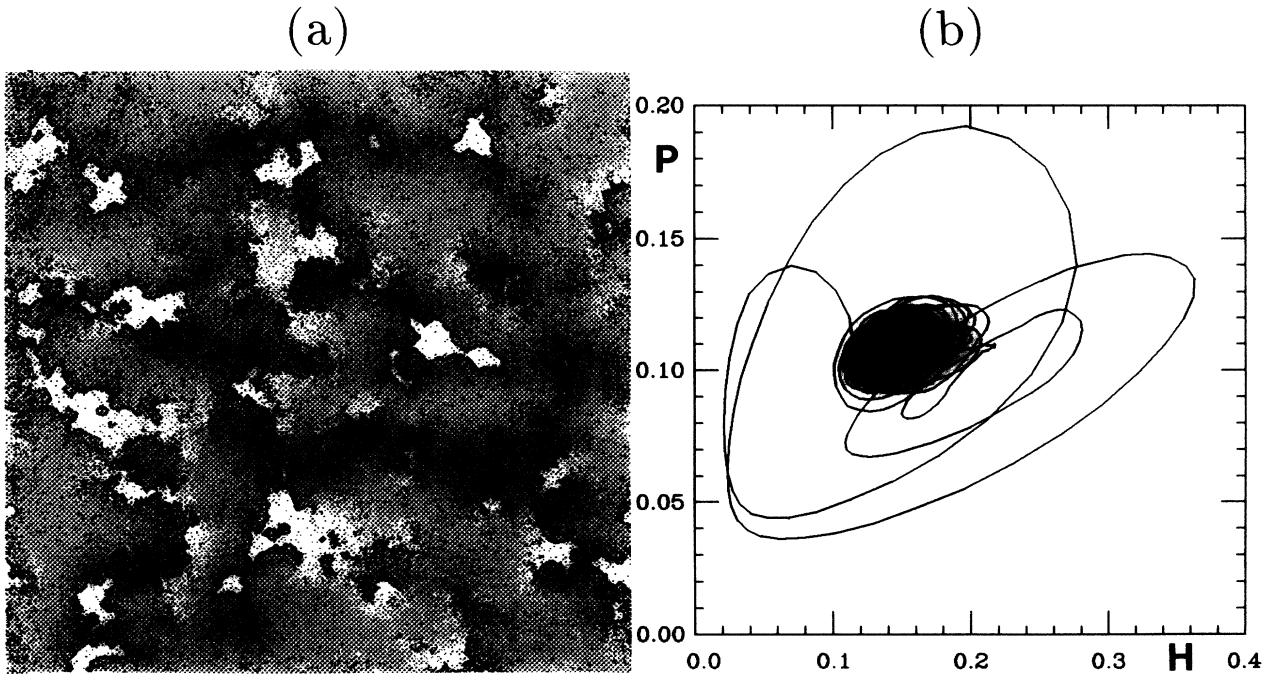

FIG. 8. Same as Fig. 6, with $m_p = m_h = 10$ and a few thousand time steps.

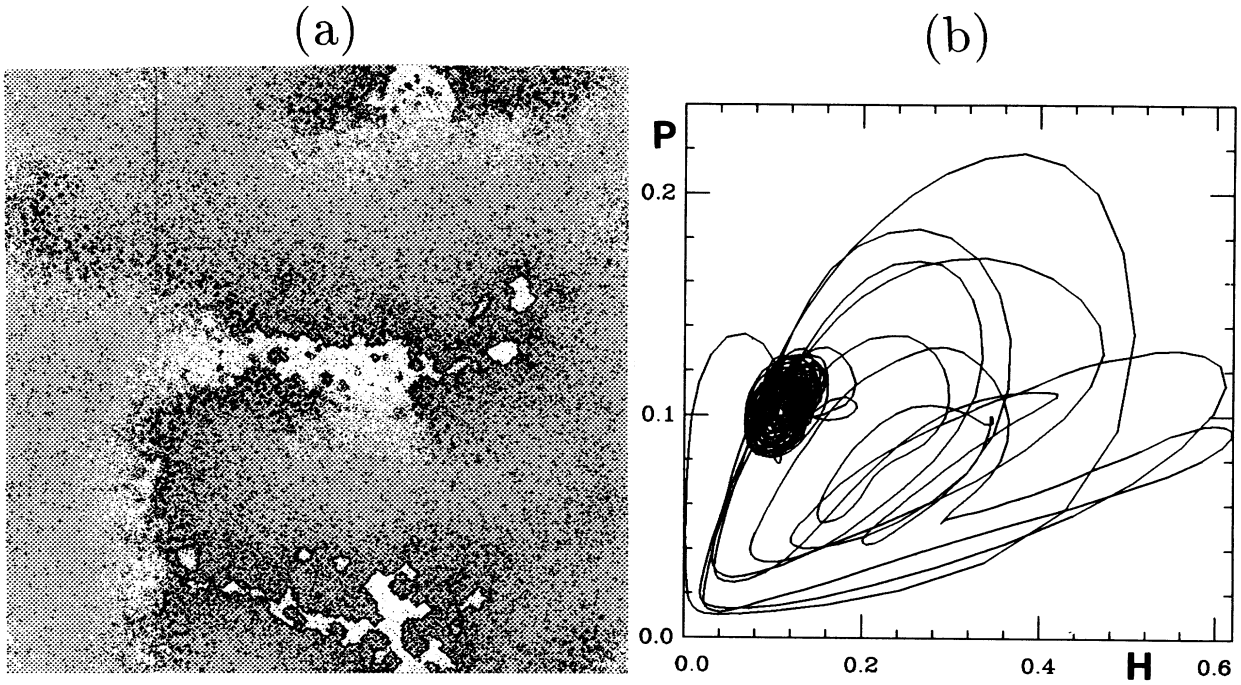

FIG. 9. Same as Fig. 6, with $m_p = m_h = 100$ and a few thousand time steps.

0.0615) is obtained for $m = 0$. At low m (i.e., $m < 0.1$), patterns obtained in the large time limit look similar to that observed in the previous case (see Fig. 6). The variations of the fixed point (H^*, P^*) as a function of $m = m_h = m_p$ are represented in Fig. 7. For $m \to 0$, $(H_0^* - H^*)$ and $(P^* - P_0^*)$ behave as m^β with $\beta \approx 0.92$ (see inset).

For large values of m_h, and m_p, patterns look completely different. Figures 8(a) and 9(a) represent typical patterns on a 512×512 site lattice obtained, respectively, for $m_h = m_p = 10$ and $m_p = m_h = 100$. Patterns are inhomogeneous with a coexistence of (i) growing prey domains with few predators and a high prey density, (ii) large clusters of preys surrounded by predators and collapsing (the preys cannot evade and will all be eaten), (iii) regions with a majority of predators dying from food scarcity. It is clear that the size of these domains increases with m.

The time evolution of predator and prey densities, starting from a random distribution with $H = P = 0.1$ look also quite different [see Figs. 8(b) and 9(b)]. There is a very long transient with large cycles and some *noisy* behavior remains in the large time limit (i.e., after a few thousands of time steps). The amplitude of this *noise* decreases if we increase the lattice size and the global densities H and P are stationary in the limit $N \to \infty$ and $t \to \infty$.

The loss of spatial coherence is generally characterized by a decay of the spatial correlations with a finite correlation length. We have measured on a 512×512 lattice the correlations functions:

$$C_h(l) = \langle [\bar{H}(i) - H][\bar{H}(j) - H] \rangle \tag{3.1}$$

$$C_p(l) = \langle [\bar{P}(i) - P][\bar{P}(j) - P] \rangle \tag{3.2}$$

where H and P are the stationary values of the global concentrations of preys and predators for $N \to \infty$; $\bar{H}(i)$ and $\bar{P}(i)$ are local concentrations measured on 8×8 squares centered at site i. The brackets represent the mean value performed on all pairs (i, j) with distance $d(i, j) = l$. To improve the statistics, our values are averages over patterns obtained during 300 time steps after

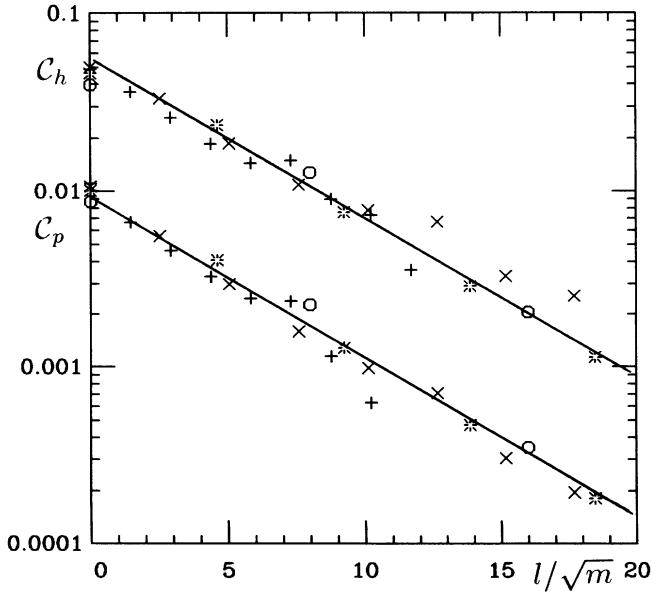

FIG. 10. Semilogarithmic plot of spatial correlation functions C_p and C_h for the local concentrations of predators and preys in terms of $l/m^{1/2}$. $\circ$: $m = 1$; $*$: $m = 3$; $\times$: $m = 10$; $+$: $m = 30$.

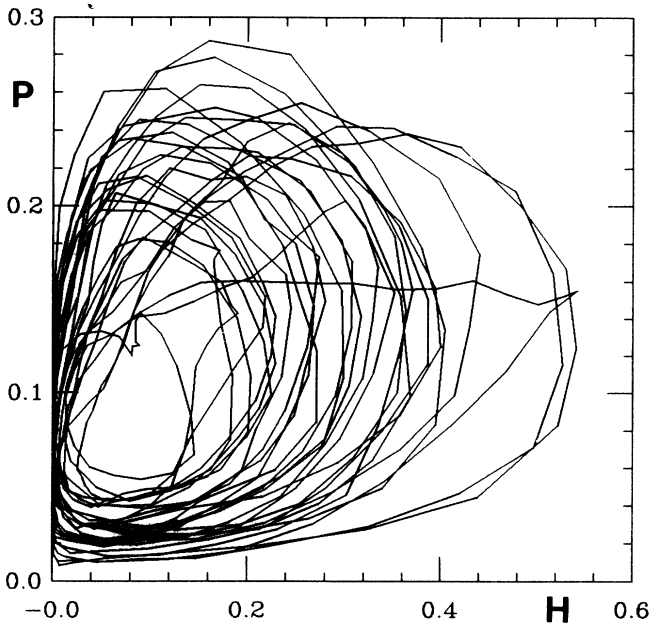

FIG. 11. Noisy cyclic behavior of the local concentrations measured on a subset of size $N' = 64 \times 64$ of a 512×512 lattice, with the parameters corresponding to Fig. 9. Four hundred iterations are shown after a transient of about one thousand time steps.

a transient of a few hundred to one thousand time steps.

A semilogarithmic plot of $\mathcal{C}_p$ and $\mathcal{C}_p$ as a function of $l/\sqrt{m}$ is represented in Fig. 10 for various $m = m_h = m_p$ ranging from 1 to 30. The correlation functions decay roughly exponentially with a correlation length $\xi \approx 4.9\sqrt{m}$.

The short-range mixing corresponds to a diffusion process which moves individuals over a distance $\sqrt{m}$ at each time step. The correlation length appears to be of the order of the "effective" range of the global rule defined for this model.

Figure 11 represents the time evolution of the local densities of predators and preys measured, for $m = 100$ on a subset of size 64×64 (i.e., roughly $\xi \times \xi$) of a 512×512 lattice. We observe a noisy cyclic behavior, while the global concentrations tend to a fixed point (see Fig. 9).

Similar behaviors with spatial disorder and stationary collective variables have been obtained in one-dimensional lattices of coupled logistic maps with periodic boundary conditions [9–11], (more striking nontrivial collective behaviors have been observed in higher dimension [12]).

We have also recently studied a simpler cellular automaton rule with short-range moves which exhibit a chaotic behavior at a local scale, while global variables are stationary [13].

For similar interaction rules with *long-range moves* (individuals move to any site chosen at random on the lattice), the behavior is different. Spatial coherence is observed ($\xi \to \infty$), while time evolution of collective variables is chaotic [13] or cyclic [14].

If the lattice size is not large enough with respect to ξ, quasicyclic behaviors may persist over many time steps. As a peculiar illustration we show in Fig. 12 the evolution of the predator and prey concentrations over 3000 time steps for a 256×256 lattice with $m_p = 30$ and $m_h = 100$.

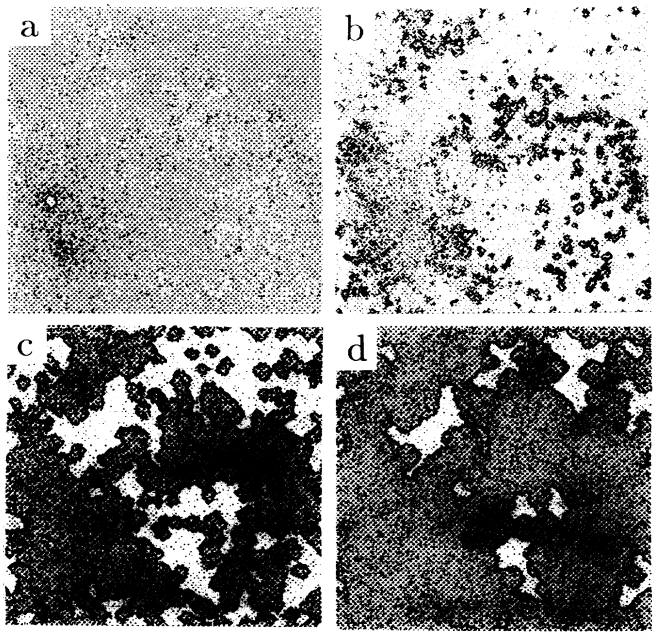

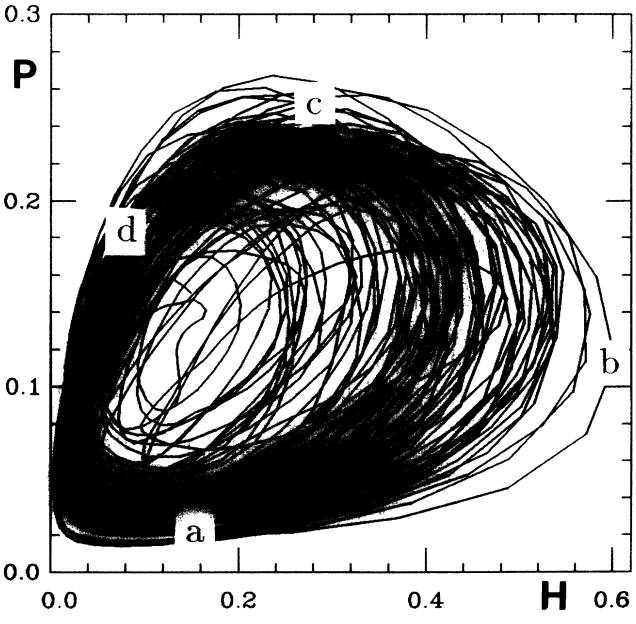

FIG. 12. Noisy cyclic behavior of the concentrations (H, P) observed over 3000 time steps on a smaller size ($N = 256 \times 256$) lattice with $m_p = 30$ and $m_h = 100$. Here $b_p = 0.6$, $d_p = 0.2$, $b_h = 0.2$, and $d_h = 0.9$. The left part of the figure illustrates four states of a cycle—see the right part—obtained after (a) 2791, (b) 2796, (c) 2802, and (d) 2807 time steps starting from equal concentrations $H_0 = P_0 = 0.1$ of preys and predators.

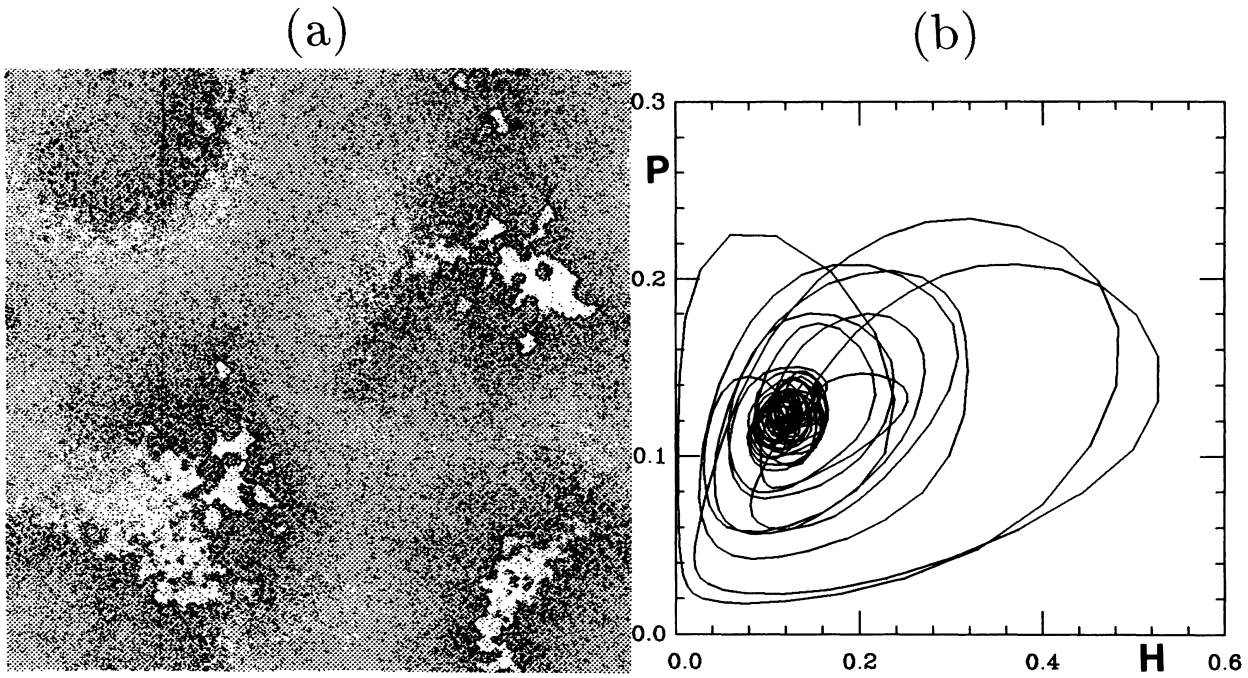

FIG. 13. Same as Fig. 6 with $m_p = 30$ and $m_h = 100$ and a few thousand time steps. Subregions corresponding to all steps of a cycle obtained on a smaller lattice (cf. Fig. 12) coexist on the pattern.

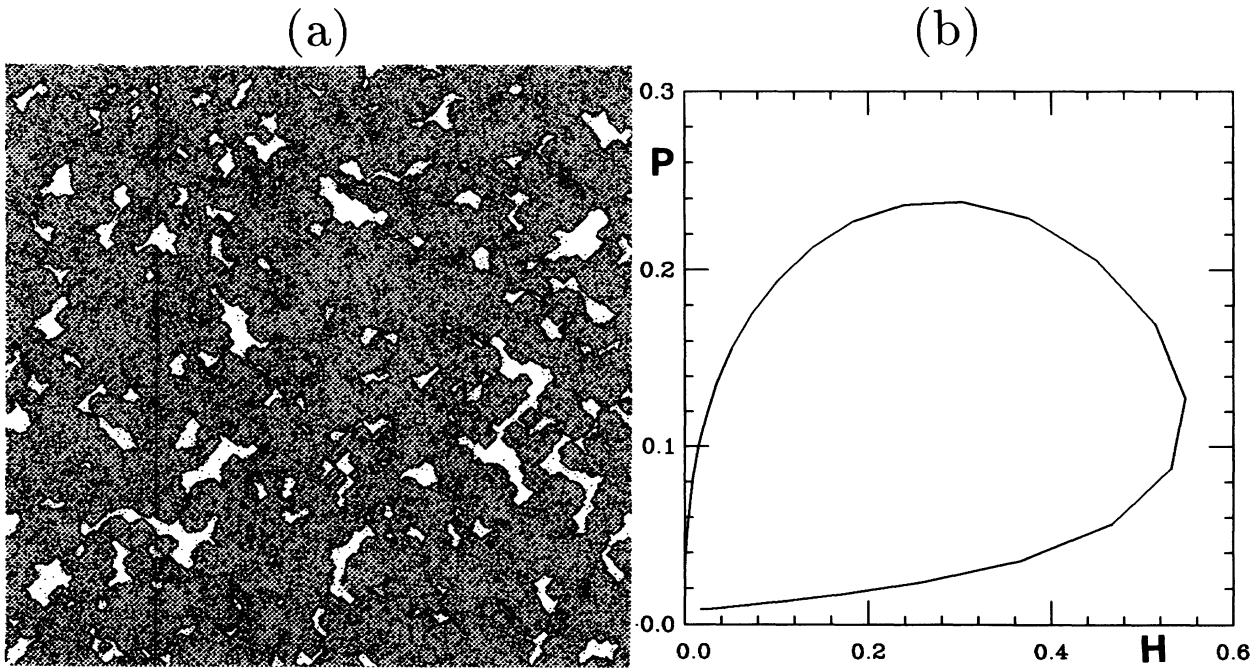

FIG. 14. Trivial fixed point ($H^* = 0, P^* = 0$) obtained with predators much faster than preys $m_p = 50$ and $m_h = 10$ and the same parameters $b_p = 0.6$, $d_p = 0.2$, $b_h = 0.2$, and $d_h = 0.9$. (a) Typical pattern after about 20 time steps starting from equal concentrations of preys and predators ($H_0 = P_0 = 0.1$) distributed at random. There only remains clusters of preys encircled by predators that prevent them from escape. (b) Time evolution of (H, P).

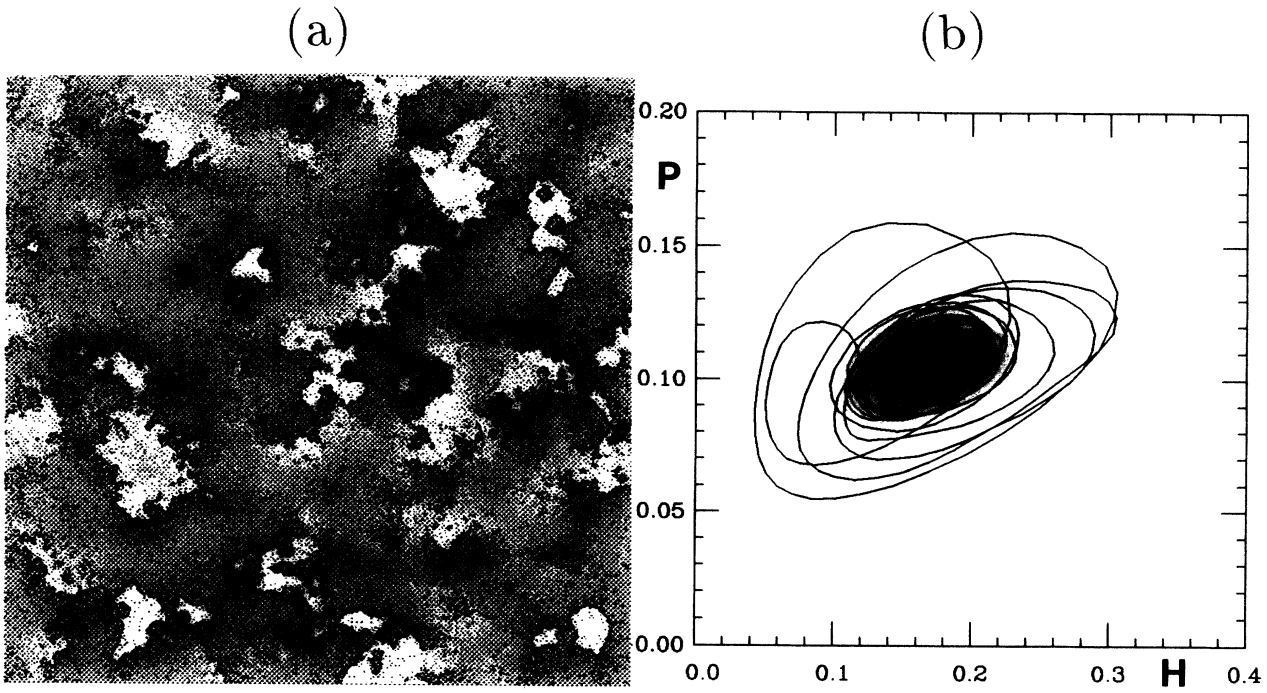

FIG. 15. Same as Fig. 6 with $b_p = 0.5$, $d_p = 0.2$, $b_h = 0.2$, $d_h = 0.9$, and $m_p = m_h = 100$ after a few thousand time steps.

For comparison, the pattern and time evolution for the same parameters on a 512×512 lattice is given in Fig. 13.

By the way, this figure shows that asymmetric moves with preys faster than predators give similar results. In contrast, if predators move faster than preys, the trivial fixed point $(H^* = 0, P^* = 0)$ can be reached. As illustrated in Fig. 14, with $m_p = 50$ and $m_h = 10$, if predators are much faster than preys, they can more easily build up compact circles around clusters of prey. When they have eaten all preys inside these clusters, they die.

Hence, with the parameter set considered in this subsection, the *qualitative* local behavior of the system in the limit $m = m_h = m_p \to \infty$ is predicted by the mean-field

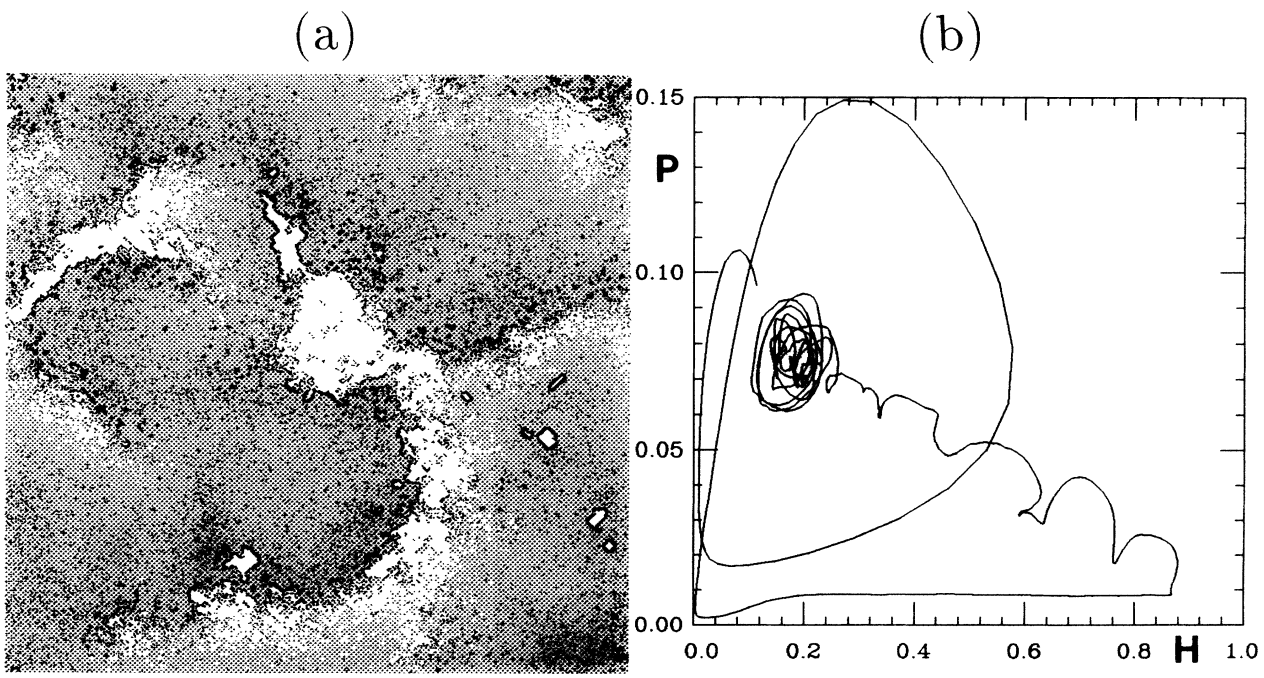

FIG. 16. (a) Typical pattern with a range $r = 2$ *pursuit-evasion* neighborhood. Here, $m_p = m_h = 100$, $b_p = 0.5$, $d_p = 0.2$, $b_h = 0.2$, and $d_h = 0.9$. (b) Corresponding time evolution of the concentrations (H, P).

approximation. However, if these four parameters b_p, d_p, b_h, d_h are close to a boundary between a fixed point and a cyclic behavior, the mean field prediction might be irrelevant.

For example with $b_p = 0.5$, $d_p = 0.2$, $b_h = 0.2$, and $d_h = 0.9$ a local cyclic behavior is still observed (see Fig. 15), while the mean-field approximation gives a fixed point.

C. Influence of the range r of the pursuit-evasion neighborhood

Qualitatively, similar behaviors have been observed with a larger range of the pursuit and evasion neighborhood: $r = 2$. As a simple illustration, we just give here the pattern obtained at large time with $b_p = 0.5$, $d_p = 0.2$, $b_h = 0.2$, $d_h = 0.9$, $m_p = m_h = 100$ (Fig. 16). There are minor differences in the patterns. For example, there are here large regions with a local prey density equal to 1. This is due to the fact that preys look at larger distances and avoid moving near a predator (see Sec. I). In a region encircled by predators, vacant sites can appear after a predator has eaten a prey but cannot diffuse within the cluster of prey. In contrast, this is possible with $r = 1$.

IV. CONCLUSION

A realistic predator-prey interaction with pursuit and evasion has been modeled using an automata network. Our simulations confirm that two-dimensional infinite systems with local interaction do not exhibit nontrivial collective behaviors [12].

In the limit of large motion rates, the mean-field approximation still provides useful qualitative—although not exact—information on the general temporal behavior of such a system as a function of the parameters.

For some parameter sets, the oscillatory behavior of the predator and prey populations predicted by the mean-field approximation is not observed for large lattices. However, an interesting behavior with quasicyclic concentrations on a scale of the order of the mean displacements of the individuals has been obtained. Cyclic behaviors which have been observed in population dynamics have received a variety of interpretations [2]. Our results suggest another possible explanation: approximate cyclic behaviors could result as a consequence of the *finite* habitat.

[1] V. Volterra, Mem. Accad. Nazionale Lincei 2, **6**, 31 (1926).
[2] J.D. Murray, *Mathematical Biology*, Biomathematics Texts Vol. 19 (Springer-Verlag, Heidelberg, 1989).
[3] S. Wolfram, Rev. Mod. Phys. **55**, 601 (1983).
[4] E. Goles and S. Martínez, *Neural and Automata Networks. Dynamical Behavior and Applications* (Kluwer, Dordrecht, 1990).
[5] N.T.J. Bailey, *The Mathematical Theory of Infectious Diseases and its Applications* (Charles Griffin, London, 1975).
[6] P. Waltman, *Deterministic Threshold Models in the Theory of Epidemics,* Lecture Notes in Biomathematics Vol. 1 (Springer-Verlag, Heidelberg, 1974).
[7] R.M. Anderson and R.M. May, *Infectious Diseases of Humans, Dynamics and Control* (Oxford University Press, Oxford, 1991).
[8] H.W. Hethcote and P. van den Driessche, J. Math. Biol. **29**, 271 (1991).
[9] K. Kaneko, Prog. Theor. Phys. (Japan) **72**, 480 (1984).
[10] T. Bohr, G. Grinstein, Y. He, and C. Jayaprakash, Phys. Rev. Lett. **58**, 2155 (1987).
[11] D.R. Rasmussen and T. Bohr, Phys. Lett. A **125**, 107 (1987).
[12] H. Chaté and P. Manneville, Prog. Theor. Phys. (Japan) **87**, 1 (1992), and references therein.
[13] N. Boccara, O. Roblin, and M. Roger (unpublished).
[14] N. Boccara and K.Y. Cheong, J. Phys. A **27**, 1585 (1993). Note that the study of this model for short-range moves is incomplete. The cycles observed in this case for concentrations of individuals are related to the finite size of the lattice. We have checked that for larger lattice sizes, global variables are stationary in the $t \to \infty$ limit.

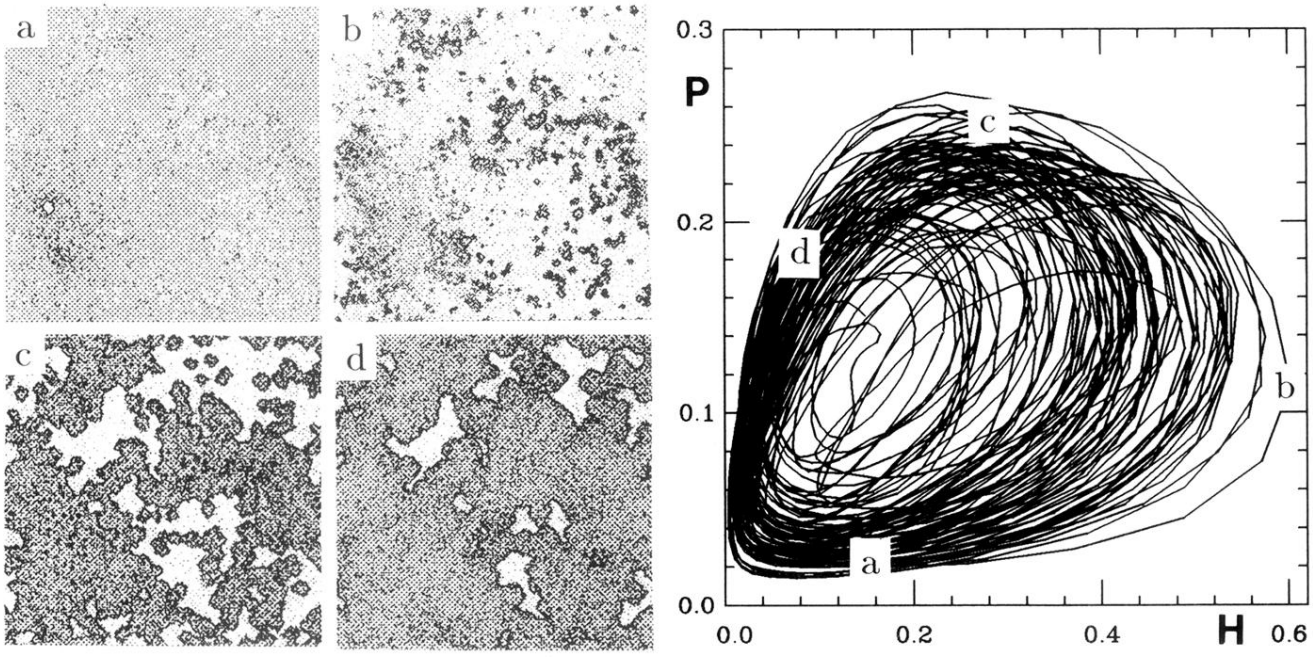

FIG. 12. Noisy cyclic behavior of the concentrations (H, P) observed over 3000 time steps on a smaller size ($N = 256 \times 256$) lattice with $m_p = 30$ and $m_h = 100$. Here $b_p = 0.6$, $d_p = 0.2$, $b_h = 0.2$, and $d_h = 0.9$. The left part of the figure illustrates four states of a cycle—see the right part—obtained after (a) 2791, (b) 2796, (c) 2802, and (d) 2807 time steps starting from equal concentrations $H_0 = P_0 = 0.1$ of preys and predators.

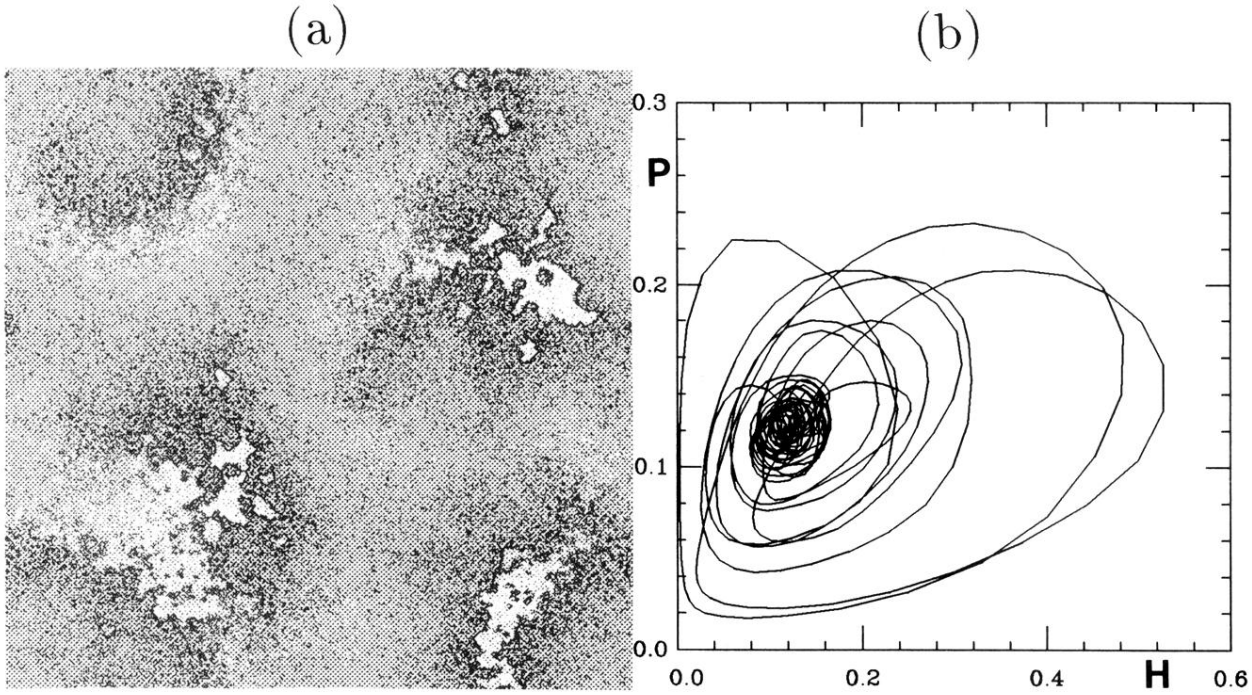

FIG. 13. Same as Fig. 6 with $m_p = 30$ and $m_h = 100$ and a few thousand time steps. Subregions corresponding to all steps of a cycle obtained on a smaller lattice (cf. Fig. 12) coexist on the pattern.

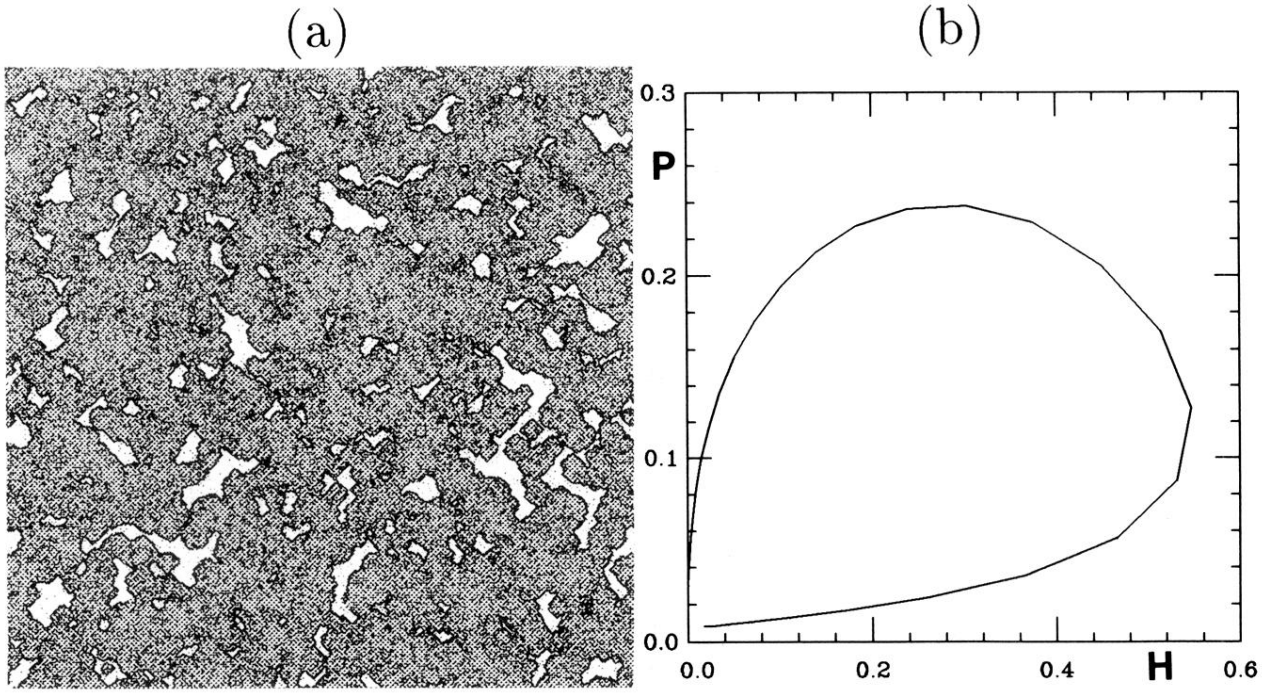

FIG. 14. Trivial fixed point ($H^* = 0, P^* = 0$) obtained with predators much faster than preys $m_p = 50$ and $m_h = 10$ and the same parameters $b_p = 0.6$, $d_p = 0.2$, $b_h = 0.2$, and $d_h = 0.9$. (a) Typical pattern after about 20 time steps starting from equal concentrations of preys and predators ($H_0 = P_0 = 0.1$) distributed at random. There only remains clusters of preys encircled by predators that prevent them from escape. (b) Time evolution of (H, P).

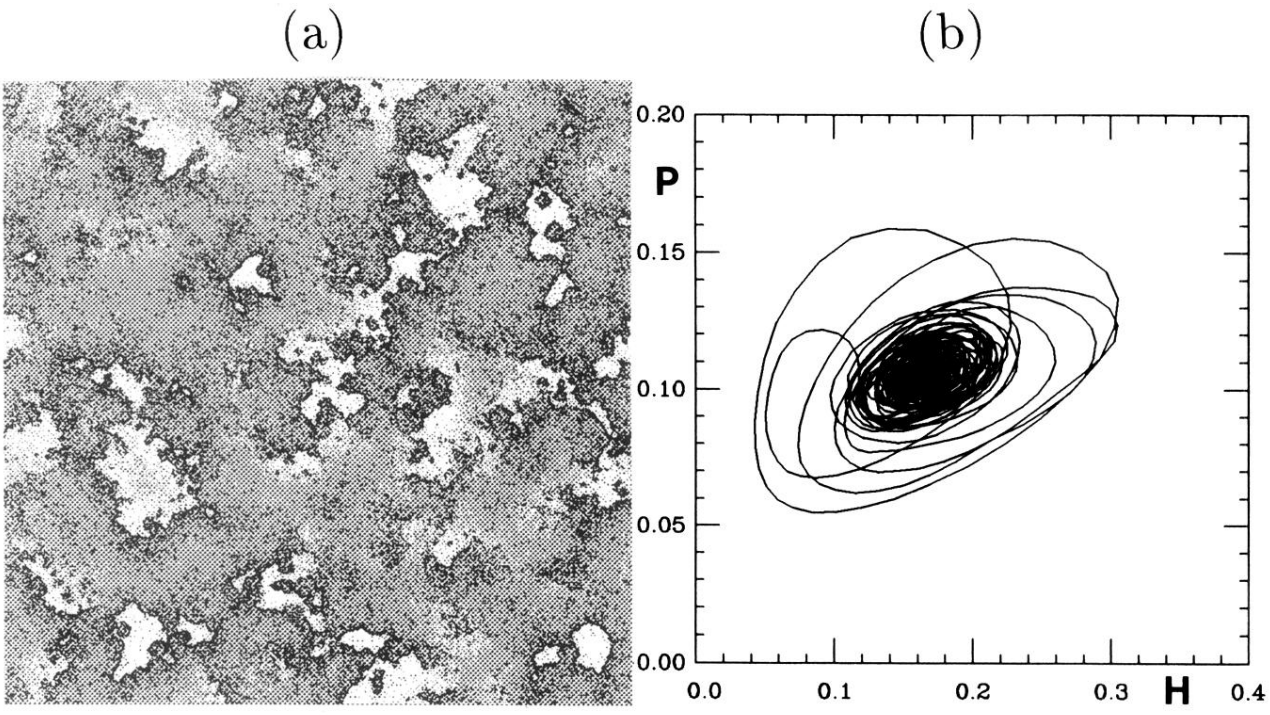

FIG. 15. Same as Fig. 6 with $b_p = 0.5$, $d_p = 0.2$, $b_h = 0.2$, $d_h = 0.9$, and $m_p = m_h = 100$ after a few thousand time steps.

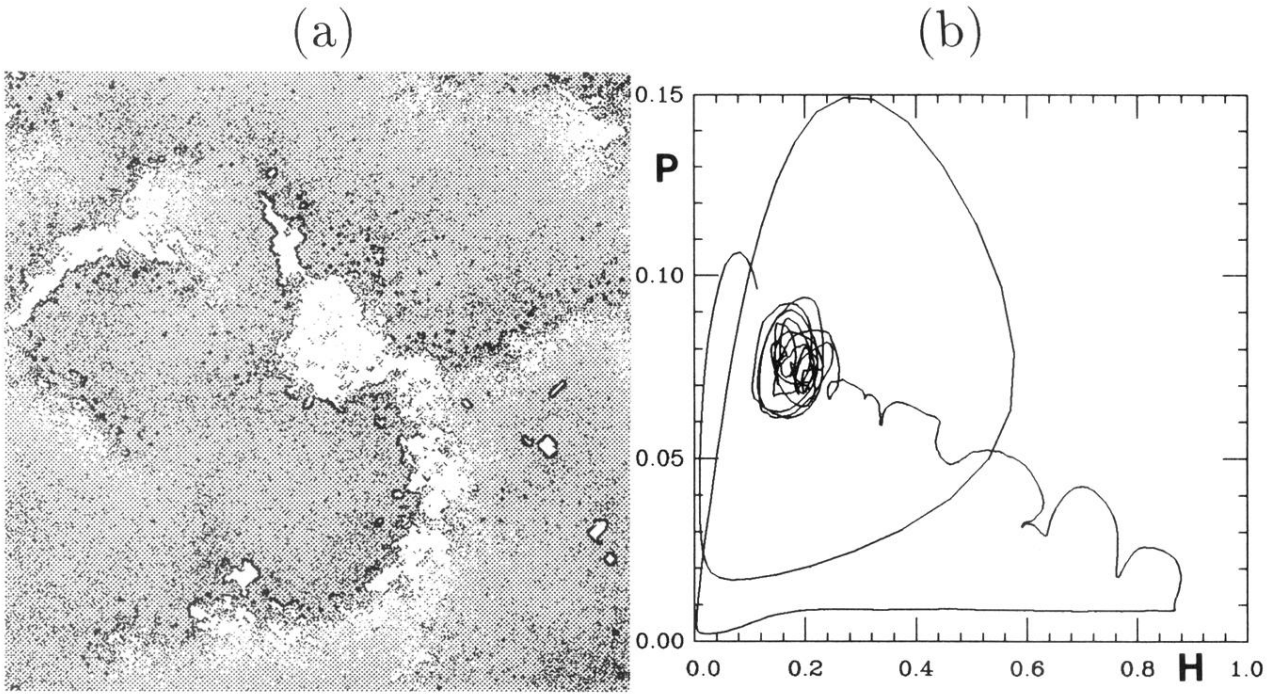

FIG. 16. (a) Typical pattern with a range $r = 2$ *pursuit–evasion* neighborhood. Here, $m_p = m_h = 100$, $b_p = 0.5$, $d_p = 0.2$, $b_h = 0.2$, and $d_h = 0.9$. (b) Corresponding time evolution of the concentrations (H, P).

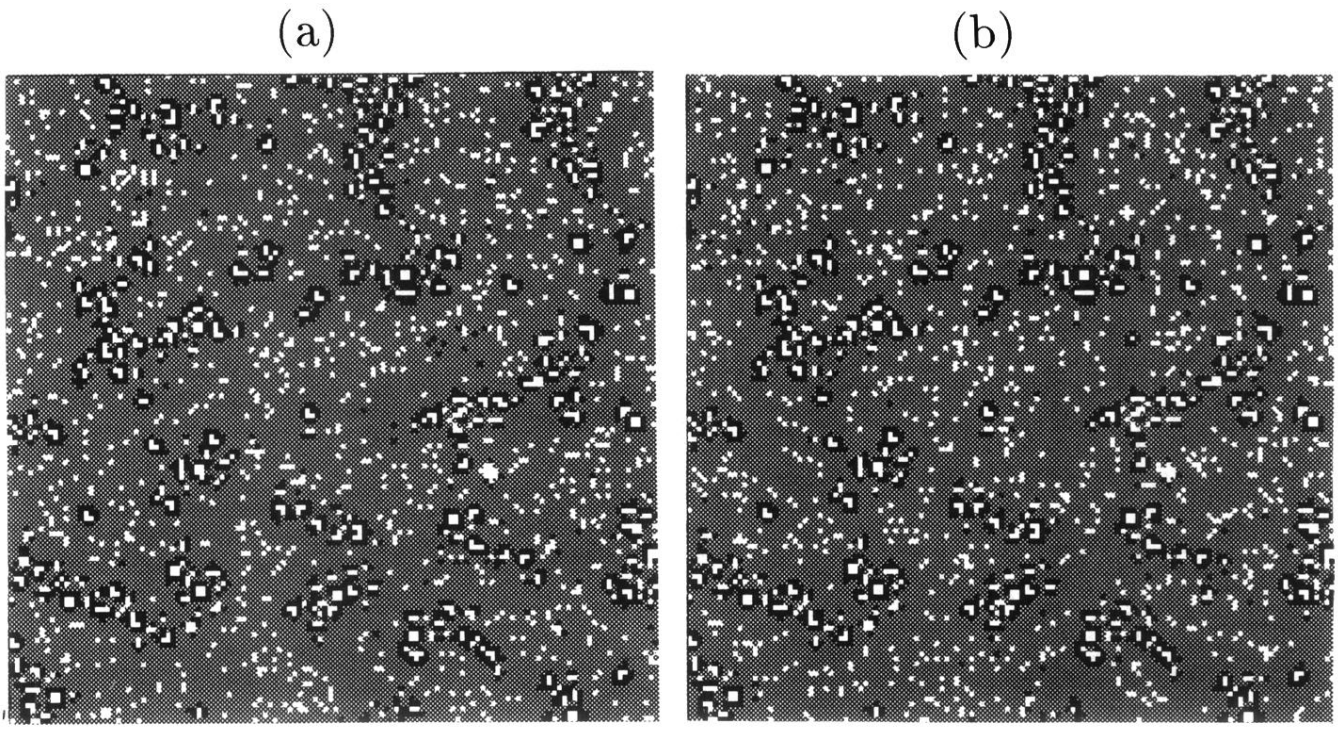

FIG. 2. Patterns obtained after 10 000 and 10 100 tentative moves of predators and preys, starting from an equal concentration $c = 10\%$ of predators and preys distributed at random. Only the *pursuit and evasion process is applied.* In all patterns, predators (respectively, preys) are represented by black (respectively, white) squares on a gray background.

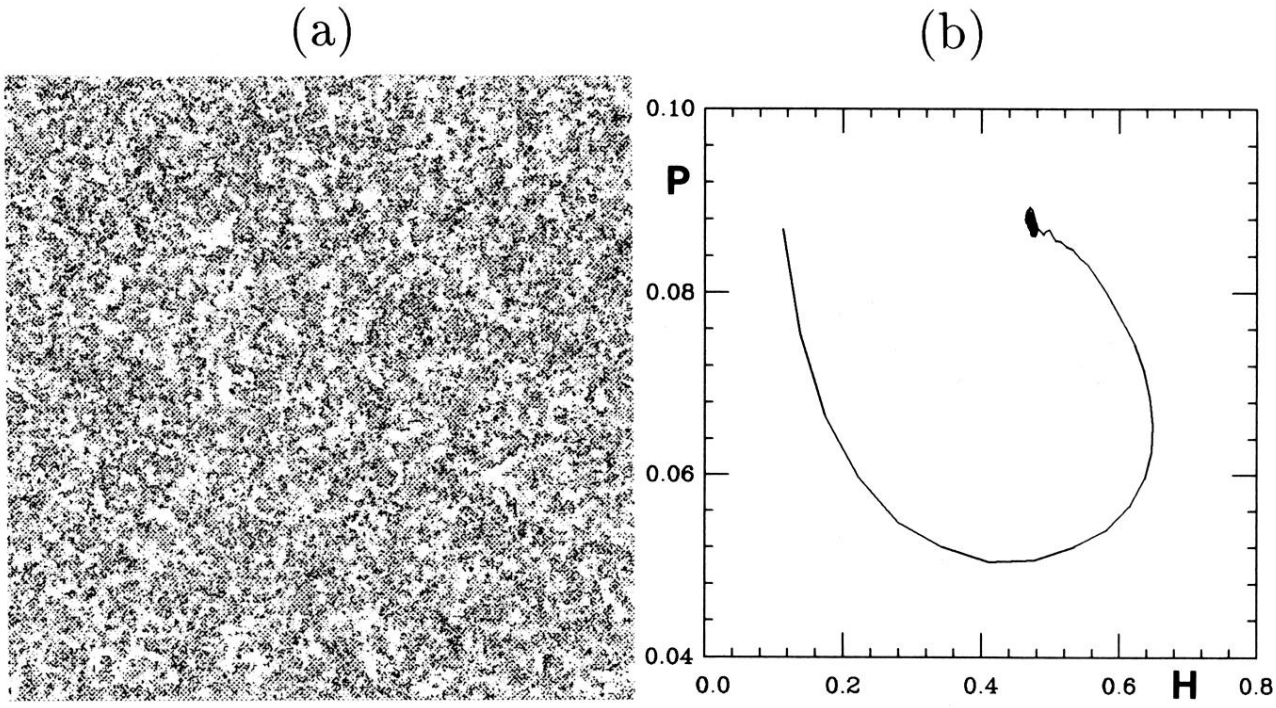

FIG. 4. (a) Patterns obtained after a few hundred time steps, starting from a random distribution of 10% of predators and 10% of preys on a 512×512 lattice with $m_p = m_h = 1$. (b) Corresponding time evolution of the densities (H, P). Here $b_p = 0.2$, $d_p = 0.2$, $b_h = 0.2$, and $d_h = 0.9$.

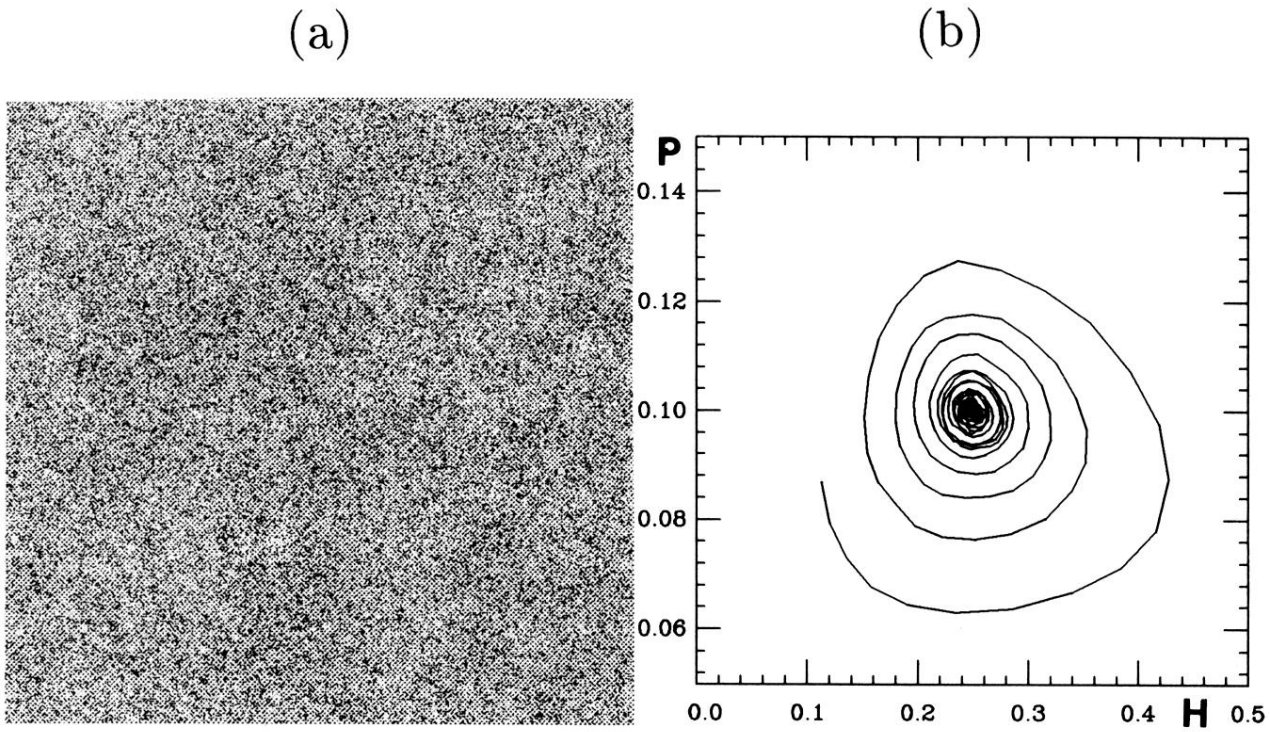

FIG. 5. Same as Fig. 4 with $m_p = m_h = 100$.

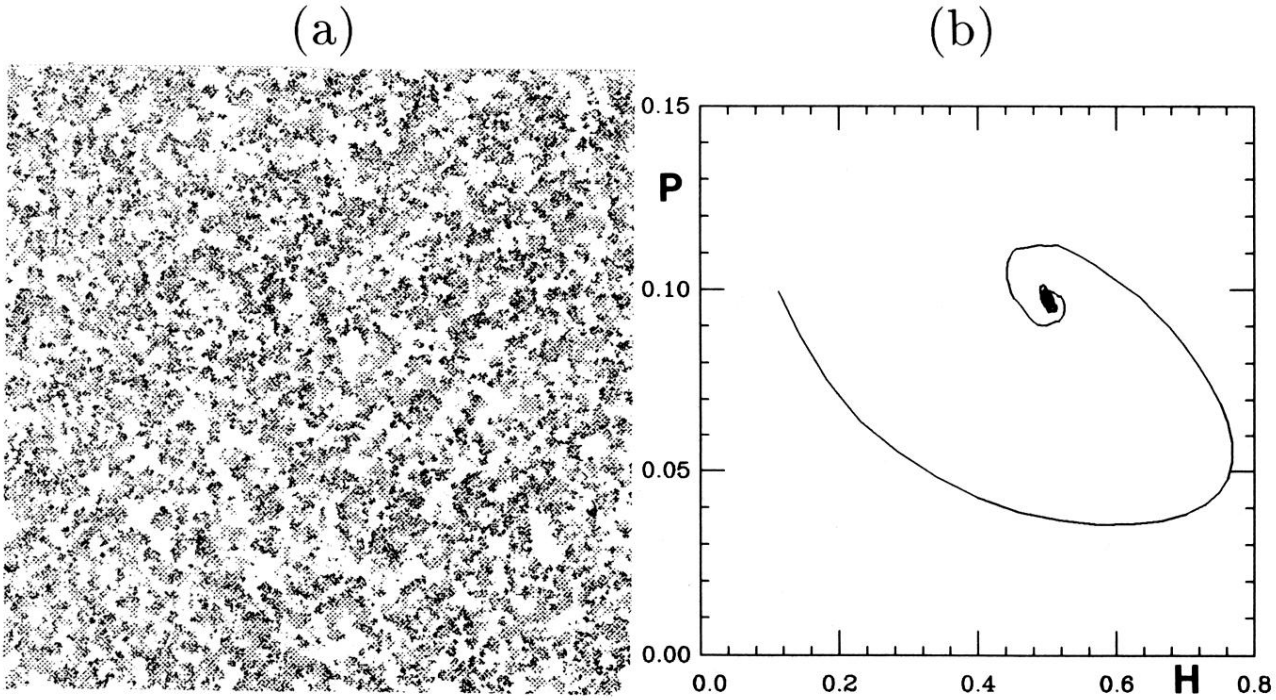

FIG. 6. (a) Pattern obtained after about a few hundred time steps, starting from a random distribution of 10% of predators and 10% of preys on a 512×512 lattice. (b) Time evolution of the densities H, P. Here $b_p = 0.6$, $d_p = 0.2$, $b_h = 0.2$, and $d_h = 0.9$; $m = m_p = m_h = 0.02$.

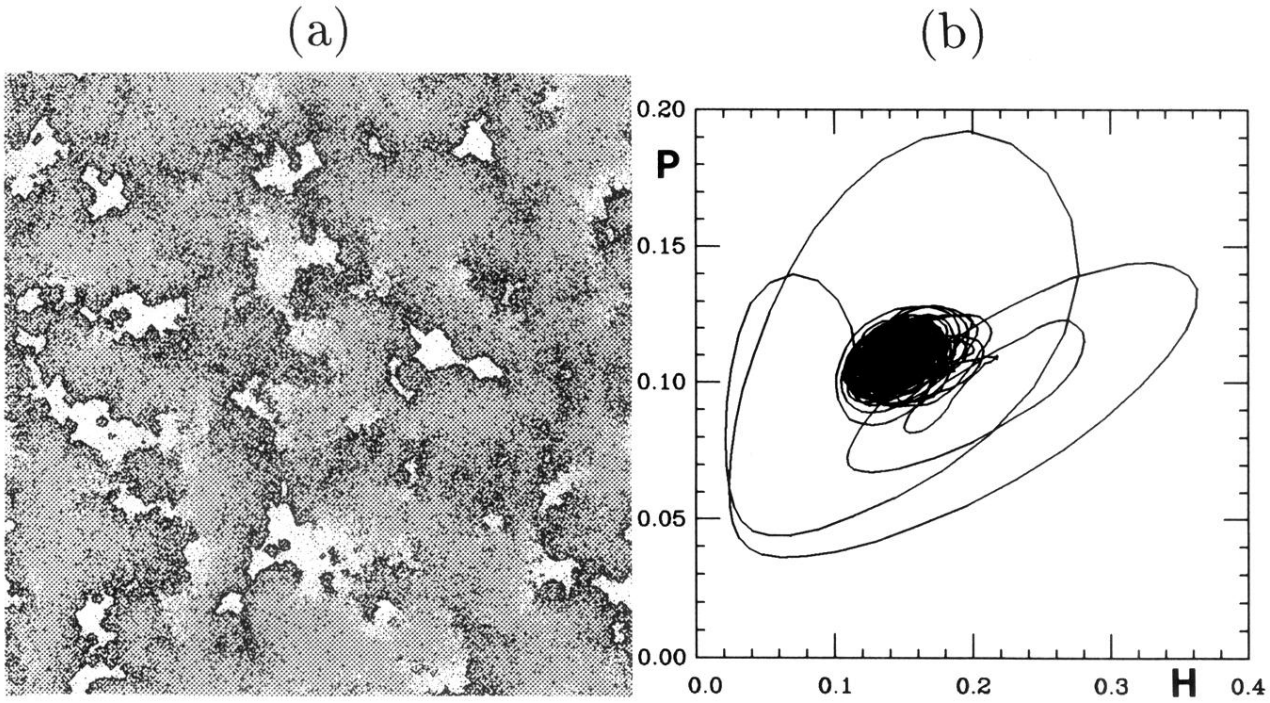

FIG. 8. Same as Fig. 6, with $m_p = m_h = 10$ and a few thousand time steps.

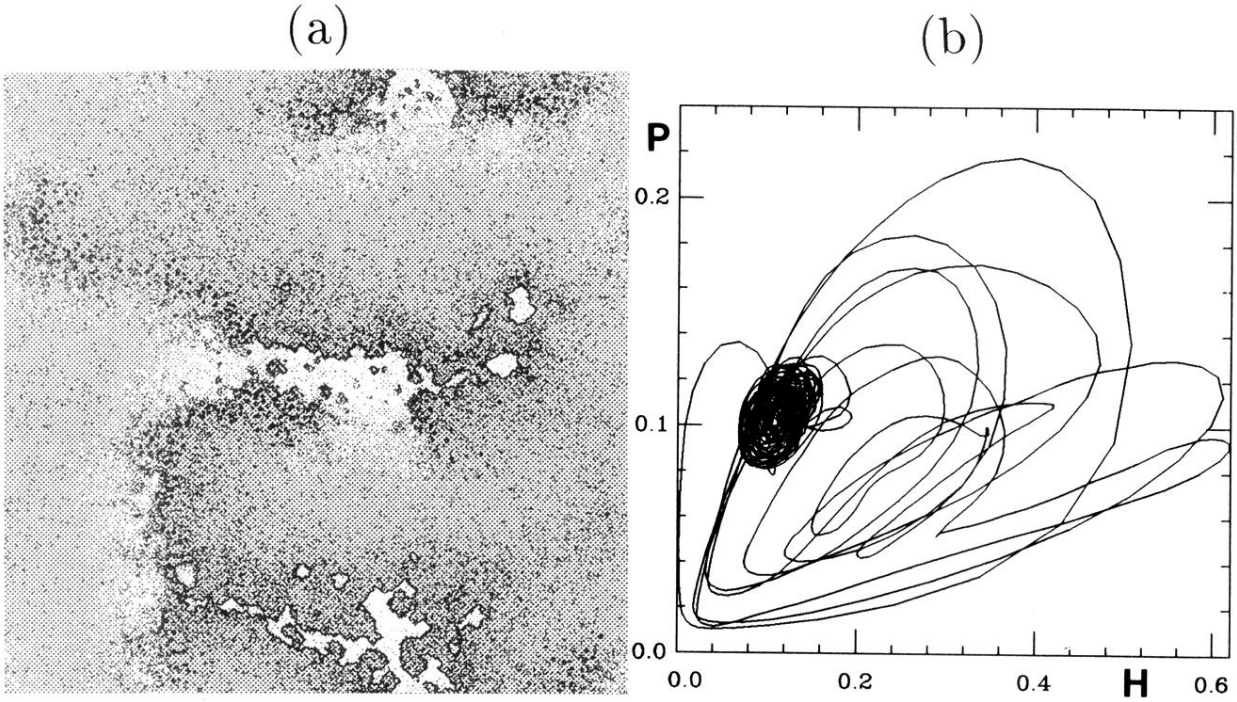

FIG. 9. Same as Fig. 6, with $m_p = m_h = 100$ and a few thousand time steps.